$t$ with the mean lifetime between jumps ($k_J^{-1}$). Taking $l \cong 5$ Å and $k_J \cong 0.2\ s^{-1}$ at room temperature gives $D \cong 4 \times 10^{-21}\ m^2\ s^{-1}$. This result is comparable with that obtained for some other compounds with similar molecular sizes.[23,24] For example, for naphthalene at room temperature $D \cong 2.5 \times 10^{-20}\ m^2\ s^{-1}$. The high activation energy determined by Maciel and co-workers[7] for the tautomeric shift reaction must therefore be ascribed to the self-diffusion process associated with the hydrogen shift (Table II).

Rotor-synchronized two-dimensional MAS exchange spectroscopy may prove useful in other solid systems where coupling between translational diffusion, chemical exchange, and molecular reorientation are involved. When the two-dimensional method is applicable, the difficulties associated with single-crystal work can be circumvented. In the following paper,[17] we describe similar investigations on solid bullvalene for which the tautomeric bond shift reaction (the Cope rearrangement) in the solid state is coupled to a molecular reorientation process. In this case, the mixing time dependence of the cross-peak intensities has been used to estimate the reaction rates and to test mechanistic proposals.

**Acknowledgment.** We thank Dr. B. Blümich for his help and interest in this research. J.J.T. thanks the Science and Engineering Research Council of Great Britain for a NATO Fellowship and Z.L. thanks the Minverva Foundation for a visiting scientist fellowship.

**Registry No.** Tropolone, 533-75-5.

(23) Sherwood, J. N. *Mol. Cryst. Liq. Cryst.* **1969**, *9*, 37.
(24) Resing, H. A. *Mol. Cryst. Liq. Cryst.* **1969**, *9*, 101.

# Solid-State Reactions Studied by Carbon-13 Rotor-Synchronized Magic Angle Spinning Two-Dimensional Exchange NMR. 2. The Cope Rearrangement and Molecular Reorientation in Bullvalene

**Jeremy J. Titman, Zeev Luz,† and Hans W. Spiess***

*Contribution from the Max-Planck-Institut für Polymerforschung, Postfach 3148, D-6500 Mainz, Germany.* *Received November 12, 1991*

**Abstract:** Carbon-13 MAS NMR measurements are reported for solid bullvalene between −40 and +85 °C. One-dimensional spectra recorded above −10 °C exhibit, as a function of increasing temperature, dynamic line broadening, followed by coalescence and, eventually, narrowing. Analysis of the line widths in the slow exchange regime indicates the presence of two independent dynamic processes: symmetric threefold jumps and bond shift tautomerism (the Cope rearrangement). Two-dimensional exchange experiments with rotor-synchronized mixing times are presented in the temperature range −20 to −10 °C with mixing times of 4–500 ms. These experiments were carried out at a slow spinning rate for which auto cross peaks between the olefinic carbon atoms as well as hetero cross peaks between the latter and the aliphatic carbons are observed. The results of these experiments are consistent with the occurrence of the two processes determined by the one-dimensional experiments and by earlier deuterium measurements and confirm that the Cope rearrangement proceeds in concert with a molecular reorientation process that preserves the crystal ordering. The estimated activation energies for the threefold jumps and the concerted Cope rearrangement/reorientation are found to be approximately 21 and 15 kcal mol$^{-1}$, respectively.

## Introduction

Bullvalene provides a unique example of the Cope rearrangement reaction. Due to the high symmetry of the molecule, more than one million (10!/3) degenerate tautomeric isomers interconvert by this process.[1] Extensive measurements of the kinetics

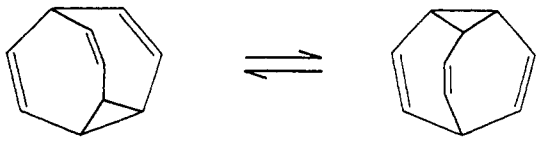

of the reaction in solution have been performed[2-6] since the first synthesis of bullvalene in 1963.[7] For many years it was thought that the Cope rearrangement could not take place in solid bullvalene since the process would perturb the crystal structure, known from X-ray and neutron diffraction to be highly ordered.[8,9] A sharp dispersion in the proton NMR second moment that occurs in solid bullvalene at around room temperature[10] was, therefore, interpreted in terms of the onset of symmetric threefold jumps of the molecules, a process that does not affect the crystal order. In 1985, however, Meier and Earl[11] showed, using carbon-13 magic angle spinning (MAS) NMR, that the observed dispersion must be due at least in part to the Cope rearrangement. They found that the resolved resonances observed for the aliphatic and olefinic carbon nuclei at low temperatures (−60 °C) coalesce and merge to a single line above room temperature. This effect can only be

† Permanent address: The Weizmann Institute of Science, Rehovot 76100, Israel.

(1) Doering, W. von E.; Roth, W. R. *Tetrahedron* **1963**, *19*, 715.
(2) (a) Saunders, M. *Tetrahedron Lett.* **1963**, *25*, 1699; (b) *Magnetic Resonance in Biological Systems*; Pergammon Press: New York, 1967; p 85.
(3) Oth, J. F. M.; Mullen, K.; Gilles, J.-M.; Schröder, G. *Helv. Chim. Acta* **1974**, *57*, 1415.
(4) (a) Gunther, H.; Ulmen, J. *Tetrahedron* **1974**, *30*, 3781. (b) Nakanishi, H.; Yamamoto, O. *Tetrahedron Lett.* **1974**, *20*, 1803. (c) Additional references in isotropic solutions of bullvalene may be found in: Mann, B. E. *Prog. Nucl. Magn. Reson. Spectrosc.* **1977**, *11*, 95.
(5) Huang, Y.; Macura, S.; Ernst, R. R. *J. Am. Chem. Soc.* **1981**, *103*, 5327.
(6) (a) Poupko, R.; Zimmermann, H.; Luz, Z. *J. Am. Chem. Soc.* **1984**, *106*, 5391. (b) Boeffel, C.; Poupko, R.; Zimmermann, H.; Luz, Z. *J. Magn. Reson.* **1989**, *85*, 329.
(7) Schröder, G. *Angew. Chem., Int. Ed. Engl.* **1963**, *2*, 481.
(8) (a) Johnson, S. M.; McKechnie, J. S.; Lin, B. T.-S.; Paul, I. C. *J. Am. Chem. Soc.* **1967**, *89*, 7123. (b) Amit, A.; Huber, R.; Hoppe, W. *Acta Crystallogr.* **1968**, *B24*, 865.
(9) (a) Luger, P.; Buschmann, J.; McMullan, R. K.; Rube, J. R.; Matias, P.; Jeffrey, G. A. *J. Am. Chem. Soc.* **1986**, *108*, 7825. (b) Luger, P.; Buschmann, J.; Richter, T.; McMullan, R. K.; Ruble, J. R.; Matias, P.; Jeffrey, G. A. *Acta Crystallogr.* **1987**, *A43*, C-105.
(10) Graham, J. D.; Santee, E. R., Jr. *J. Am. Chem. Soc.* **1966**, *88*, 3453.
(11) Meier, B. H.; Earl, W. L. *J. Am. Chem. Soc.* **1985**, *107*, 5553.

0002-7863/92/1514-3765$03.00/0 

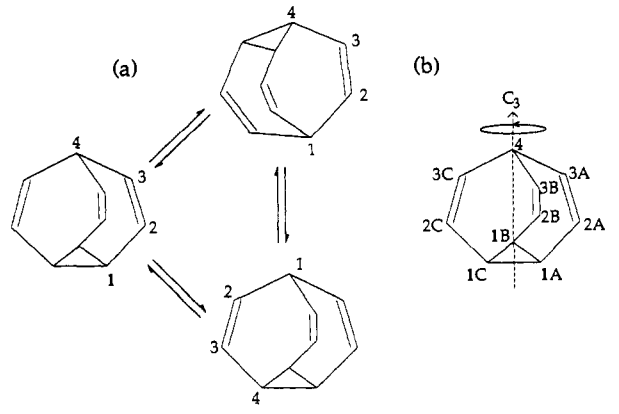


**Figure 1.** Schematic representations of (a) the concerted Cope rearrangement/reorientation process and (b) the symmetric threefold jumps that occur in solid bullvalene. In (a), the upper-left edge of the triangle represents the bond shift step and the right arm the concomitant reorientation, which restores the molecule to its original orientation. The pathway of four of the carbon atoms for this particular sequence of bondshift/reorientation is indicated. In (b) the $C_3$-axis about which the threefold jumps take place is shown. Also indicated is the numbering convention used in the present work: the three-membered ring carbons 1, the olefinic carbons 2 and 3, and the bridgehead carbon 4. Carbons 1, 2, and 3 are further classified according to the wings A, B, and C to which they belong. Wing A lies in the plane defined by the molecular fixed coordinates 1 and 3 while wings B and C are rotated by respectively ±120° about the molecular 3-axis.

explained in terms of the Cope rearrangement, which interchanges all the carbon species in the molecule. To account for the observed high order of bullvalene crystals, Meier and Earl proposed[11] that this tautomeric bond shift reaction involves a concomitant reorientation which restores the molecule to its original orientation (see Figure 1a). However, no quantitative analysis was given which would confirm the mechanism or provide rate constants for the reaction, nor was the question of the occurrence of the threefold jump process resolved.

The problem was recently addressed again using deuterium NMR of a single crystal of bullvalene-$d_{10}$.[12] The results of this work confirmed the proposed concerted mechanism and allowed the determination of the rate constant of the rearrangement over a wide temperature range. It was also found that the molecules do indeed undergo symmetric threefold jumps independent from the concerted reaction and with different kinetic parameters. In the present work, we study the solid bullvalene system using a completely different approach, employing carbon-13 MAS experiments on powder samples in one and two dimensions. The one-dimensional experiments employed were conventional cross polarization (CP) MAS measurements[13] performed at a spinning rate, $\omega_R$, slow relative to the chemical shift anisotropy, $\omega_L\Delta\sigma$, so that information about pure reorientation processes was retained in the spectrum. Although a complete analysis over the full temperature range in terms of the two dynamic processes described above can in principle be performed,[14] we limit ourselves here to the slow exchange regime where suitable equations can be used to obtain approximate values for the rate parameters. The two-dimensional experiments consisted of the rotor-synchronized modification[15,16] of the conventional two-dimensional exchange experiment.[17] As for the one-dimensional case, when the sample spinning frequency is smaller than the chemical shift anisotropy, information about molecular reorientation can be retrieved from the results, thus providing a more complete picture of the reaction pathway. A detailed description of this two-dimensional rotor-synchronized MAS exchange experiment with the relevant theory applicable to exchange between different carbon atoms may be found in the preceding paper (hereafter referred to as paper 1).[18] In that paper, we investigated the mechanism of the self-diffusion in tropolone using the cross-peak pattern observed at long mixing times, while, in the present work, we demonstrate the feasibility of the method for the study of both kinetic parameters and mechanisms from a series of such experiments on bullvalene recorded as a function of the mixing time.

## Experimental Section

Bullvalene in powder form was kindly provided by Prof. G. Schröder of Karlsruhe University. In order to shorten the long spin–lattice relaxation times in the solid the sample used for the two-dimensional experiments was exposed to a 750-kGy dose of electron irradiation and kept at 4 °C between measurements. Even then recycle times of 30 s were required for measurements below 0 °C. For the one-dimensional experiments a nonirradiated sample was used with recycle times ranging from 30 s at 85 °C to 100 s at −20 °C.

Carbon-13 CPMAS spectra were recorded on a Bruker MSL 300 spectrometer at 75.47 MHz. The dry nitrogen gas used to spin the rotor also served for cooling or heating the sample to the desired temperature. The gas temperature was monitored by a thermocouple just outside the rotor system to an estimated accuracy of ±2 °C in the region 0–40 °C. Outside this temperature range the error may be somewhat larger. The two-dimensional spectra were acquired using the pulse sequence discussed in paper 1 and processed according to the method of Hagemeyer et al.[17] in order to obtain pure absorptive spectra. The experimental details are given in the relevant figure captions.

## One-Dimensional CPMAS Spectra

The one-dimensional CPMAS measurements of Meier and Earl were extended in order to better define the temperature range over which the dynamic line broadening occurs and to acquire sufficient data to allow an estimate of the rate parameters. Examples recorded at spinning frequencies around 4 kHz over the temperature range −20 to +85 °C are shown in Figure 2. The spectrum at the lowest temperature shows well-resolved peaks due to the aliphatic carbons 1 and 4 at respectively 22 and 31 ppm (relative to TMS) and a further peak at 128 ppm due to the unresolved olefinic carbons 2 and 3 flanked by spinning sidebands. The spectrum remains unchanged on further cooling below −20 °C but as may be seen in the figure it undergoes noticeable changes on heating.

Above −20 °C the peaks in the spectrum broaden and eventually merge into a single narrow line reflecting the effect of the Cope rearrangement (Figure 1a). Closer examination of spectra taken at small temperature intervals (not all shown in Figure 2) indicate, however, that the initial broadening of the different lines is not the same. This suggests the occurrence of another process, which can be identified as the symmetric threefold jumps (Figure 1b) known to occur in solid bullvalene from deuterium NMR measurements.[12] In Figure 3 the measured half-width at half-maximum intensity, $\Delta = 1/T_2$, of the different center bands is plotted in the temperature region for which the lines are at least partially resolved. To obtain these data above 0 °C the measurements were made on traces recorded without exponential broadening, allowing measurements to be made up to +15 °C. Also plotted in Figure 3 is the half-width of the coalesced peak in the high-temperature region of the measurements. All the results in this figure are corrected to a common exponential broadening factor of 80 Hz.

Below −20 °C line line widths are essentially constant although they are different for different carbon atoms. The relatively large value for the olefinic peak can be at least partly ascribed to the small isotropic chemical shift difference between carbons 2 and 3. Above −20 °C, the initial broadening of the peaks due to the aliphatic carbon 1 and the olefinic carbons is similar, whereas that of carbon 4, the bridgehead carbon, is much less. If the broadening

(12) Schlick, S.; Luz, Z.; Poupko, R.; Zimmermann, H. *J. Am. Chem. Soc.*, submitted for publication.
(13) Schaefer, J.; Stejskal, E. O. *J. Am. Chem. Soc.* **1976**, *98*, 1031.
(14) Schmidt, A.; Vega, S. *J. Chem. Phys.* **1987**, *87*, 6895.
(15) (a) de Jong, A. F.; Kentgens, A. P. M.; Veeman, W. S. *Chem. Phys. Lett.* **1984**, *109*, 337. (b) Kentgens, A. P. M.; de Jong, A. F.; de Boer, E.; Veeman, W. S. *Macromolecules* **1985**, *15*, 1045. (c) Kentgens, A. P. M.; de Boer, E.; Veeman, W. S. *J. Chem. Phys.* **1987**, *87*, 6859.
(16) Hagemeyer, A.; Schmidt-Rohr, K.; Spiess, H. W. *Adv. Magn. Reson.* **1989**, *13*, 85.
(17) Ernst, R. R.; Bodenhausen, G.; Wokaun, A. *Principles of Nuclear Magnetic Resonance In One and Two Dimensions*; Clarendon Press: Oxford, 1987; Chapter 9.
(18) Titman, J. J.; Luz, Z.; Spiess, H. W. *J. Am. Chem. Soc.*, preceeding paper in this issue.

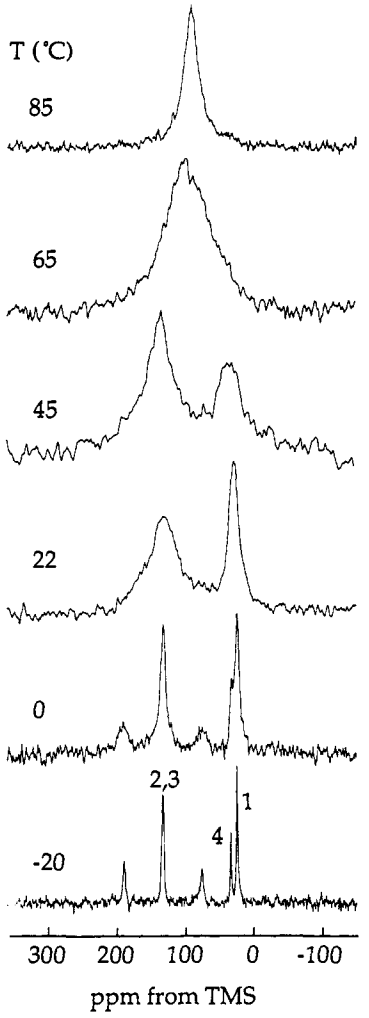


**Figure 2.** Carbon-13 CPMAS NMR spectra of solid bullvalene at different temperatures as indicated: spinning rate 4 kHz, CP contact time 800 μs, recycle delay varying from 100 s at −20 °C to 30 s at +85 °C. The number of coadded signals ranged from 64 to 1000 with larger numbers used for the broader spectra around +30 °C. The time domain data were multiplied by an exponential filter before Fourier transformation with 80-Hz line broadening except for the spectra around +30 °C, which were broadened by 200–400 Hz.

were solely due to the Cope rearrangement, the initial effect would be nearly the same for all the peaks, while, if it were solely due to the threefold jump process, carbon 4 would be unaffected. We thus identify the broadening of the carbon 4 peak with the effect of the Cope rearrangement and the broadening of the other peaks to the total effect of this and the threefold jump process.

To derive approximate values for the two rate constants from the initial line broadening we can use the equations for dynamic MAS spectra in the slow exchange limit defined by

$$W < \omega_R \lesssim \omega_L\Delta\sigma \quad \text{or} \quad W < \omega_R,\omega_L\delta\sigma \tag{1}$$

where $W$ is the overall rate of the reactions, $\omega_R$ the spinning frequency, $\omega_L\Delta\sigma$ the chemical shift anisotropy, and $\omega_L\delta\sigma$ the isotropic chemical shift difference between exchanging carbon atoms. Under these conditions, the exchange-broadened line width is given by[14]

$$\Delta = 1/T_2^0 + W \tag{2}$$

where $1/T_2^0$ is an exchange-independent line width. In this limit

$$\Delta(4) = 1/T_2^0(4) + k_C \tag{3}$$

for carbon 4 and

$$\Delta(2,3) = 1/T_2^0(2,3) + (1 - \tfrac{2}{9})k_C + k_J \tag{4}$$

for the olefinic carbons where $k_C$ and $k_J$ are the rate constants

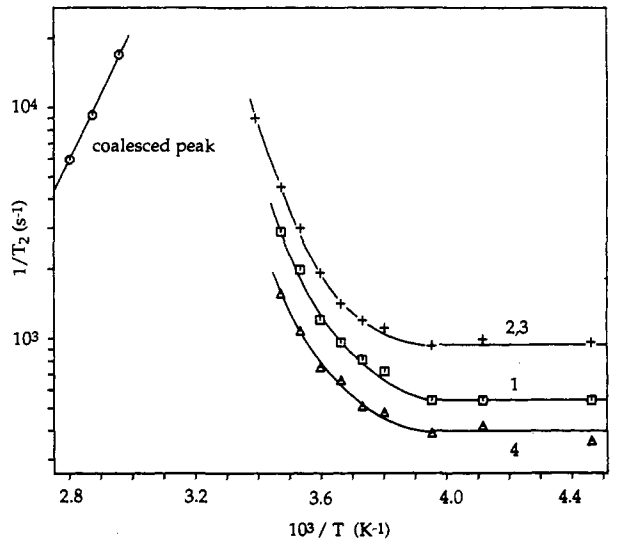


**Figure 3.** Half-width at half-height, $\Delta = 1/T_2$, of the resolved center bands for carbons 1, 2, 3, and 4 in the CPMAS NMR spectra of bullvalene in the slow exchange regime (<20 °C) and of the coalesced peak in the fast exchange regime (>60 °C), plotted as a function of the reciprocal absolute temperature. All line widths include a common exponential line broadening factor of 80 Hz.

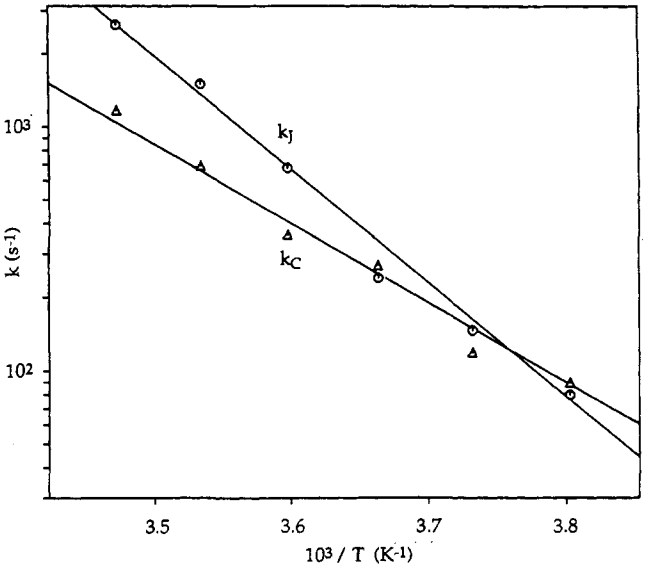


**Figure 4.** Arrhenius plots of the estimated rate constants for the Cope rearrangement and the threefold jump process in solid bullvalene. The results were derived from the initial broadening (see Figure 3) of the center bands due to carbon 4 and the olefinic carbons 2 and 3 using the slow exchange approximation.

for the Cope rearrangement and the threefold jumps, respectively. The factor $^2/_9$ in eq 4 accounts for the average probability that an olefinic carbon atom is not affected by the Cope rearrangement (see below). A similar equation may also be written for carbon 1 but because of its smaller chemical shift anisotropy this has a narrower range of validity. Using eqs 3 and 4 and the experimental line widths of carbons 2, 3, and 4 in the slow exchange regime, we can estimate values for $k_C$ and $k_J$. In practice $1/T_2^0$ was taken as the average low-temperature limiting value: 960 s$^{-1}$ for the olefinic carbon atoms and 390 s$^{-1}$ for carbon 4 (see Figure 3). The results for $k_C$ and $k_J$ obtained in this fashion are plotted in Figure 4 against reciprocal absolute temperature, yielding activation energies of 15 and 21 kcal mol$^{-1}$ for the Cope rearrangement and the threefold jumps, respectively.

### Rotor Synchronized Two-Dimensional Exchange Experiments

The one-dimensional MAS spectra of bullvalene in the slow exchange regime are not very sensitive to the mechanistic pathway

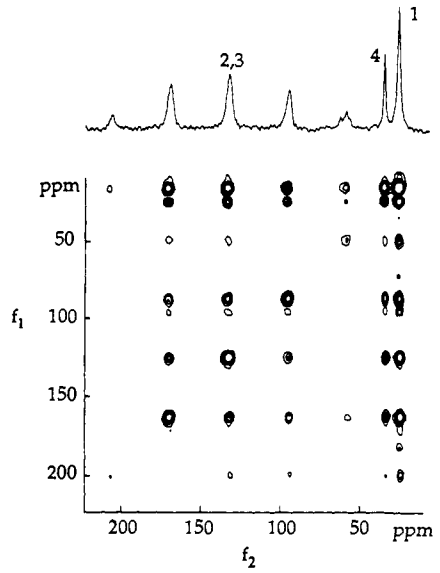


**Figure 5.** Carbon-13 two-dimensional MAS exchange spectrum of bullvalene obtained with a rotor-synchronized mixing time of 60 ms at −20 °C and rotor spinning frequency of 2.8 kHz. The carbon and proton $\pi/2$ pulse lengths were 3.8 μs. The CP contact time was 800 μs and the recycle delay was 30 s. The spectral width in both dimensions was 22.7 kHz. Data were acquired for 11.2 ms in $t_2$ and the maximum value of $t_1$ was 2.8 ms. A one-dimensional spectrum recorded under the same conditions is shown parallel to $f_2$.

of two reactions. More detailed information can be obtained by using a two-dimensional exchange experiment under conditions of slow MAS ($\omega_R < \omega_L\Delta\sigma$) with a rotor-synchronized mixing time. As indicated before a detailed description of the method is included in paper 1 and will not be repeated here. An example of such a spectrum for bullvalene recorded at −10 °C and with a spinning frequency of 2.8 kHz is shown in Figure 5 along with the corresponding one-dimensional spectrum. Essentially all the diagonal peaks are linked to each other by exchange cross peaks, indicating the effect of the Cope rearrangement, which interchanges all carbon atoms in the molecule. Whether the molecules independently undergo the threefold jumps can only be determined by a quantitative analysis of the peak intensities as a function of mixing time. Note that, at the chosen spinning frequency, there are no observable sidebands for the aliphatic carbons 1 and 4, whereas two pairs of spinning sidebands are seen for the olefinic carbons 2 and 3. For the discussion below it is convenient to classify the observed peaks into four catagories: (1) the diagonal peaks due to the aliphatic carbons 1 and 4, (2) the diagonal peaks (both center bands and sidebands) due to the olefinic carbons 2 and 3, (3) the hetero cross peaks linking the aliphatic carbons 1 and 4 with each other and with the sidebands of the olefinic carbons, and (4) exchange cross peaks linking the different sidebands of the olefinic carbon resonances. The peaks in group 3 predominantly reflect the Cope rearrangement and their intensites contain information about the nature of the concerted reorientation, while those in group 4 reflect both the threefold jump process and the Cope rearrangement because both contribute to the reorientation of the olefinic carbon atoms.

The relative intensities of the peaks depend on a number of parameters including the chemical shift tensors of the exchanging nuclei, the exact kinetic pathways of the reactions, their rate constants, and the mixing time used to record the spectrum. Thus, by a comparison of the experimental evolution of the intensities as a function of mixing time with model calculations, the kinetic parameters and the mechanisms of the reactions can be determined. Rather than analyze the whole set of peaks individually, we discuss the total intensities for each of the four groups classified above. A set of results obtained at −10 °C and a spinning frequency of 2.8 kHz is plotted in Figure 6 as a function of the mixing time in the range 4–150 ms. Note, in particular, the marked nonmonotonic behavior of the curve for group 4. In the following

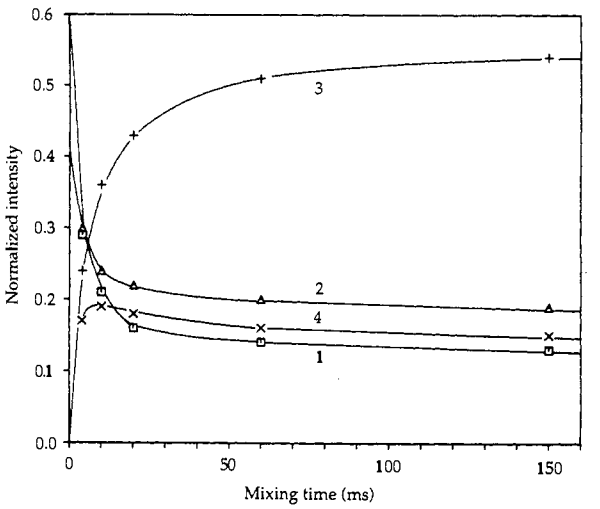


**Figure 6.** Relative intensities normalized to a total of unity of groups of peaks in the two-dimensional exchange NMR experiment at −10 °C as a function of the mixing time, $\tau_m$, in the range 4–150 ms: (1) the diagonal peaks due to carbons 1 and 4, (2) the diagonal center band and sideband peaks of carbons 2 and 3, (3) the exchange cross peaks linking carbons 1 and 4 with each other and with the sidebands of carbons 2 and 3, and (4) the cross peaks linking different sidebands of carbons 2 and 3. The points are experimental data and the lines are drawn to guide the eye. All the two-dimensional datasets recorded to produce this figure were acquired in the same total time of 13 h and processed in an identical fashion. The parameters are the same as for Figure 5 except for the temperature and that the maximum value of $t_1$ was 2.1 ms.

sections, the basic equations necessary for the calculation of intensities as a function of mixing time are described with specific reference to the case of bullvalene and the results of such calculations are then compared with the experimental data of Figure 6. Before doing so, two points need to be considered. The first concerns the cross-polarization efficiency. If this is not the same for all the carbon atoms in the system, the calculations become complicated by the necessity to use nonstoichiometric initial magnetizations. For the present work, we found this not to be necessary, since the relative integrated intensities of the carbon resonances in the one-dimensional spectra of bullvalene obtained by CPMAS were very close to their expected stoichiometric ratios. In addition, the two-dimensional spectra appear to be symmetric about the main diagonal. Both these observations indicate that the cross-polarization efficiency for all the carbon atoms is similar. The second point concerns the possible contribution of spin diffusion to the cross-peak intensities. This is known to occur in molecular crystals but normally requires a time scale of several seconds or longer.[19] In contrast, the main dynamic effects in our experiments occur in less than one-tenth of a second and we can safely neglect spin diffusion effects in our analysis.

### Calculation of Intensities of Two-Dimensional MAS Exchange Spectra as a Function of Mixing Time

As shown in paper 1, the time domain signal of a two-dimensional rotor-synchronized MAS exchange experiment, $S(t_1,t_2;\tau_m)$, consists of the weighted sum

$$S(t_1,t_2;\tau_m) = \sum_{i,j} P_{i,j}(\tau_m) S_{i,j}(t_1,t_2) \qquad (5)$$

where $P_{i,j}(\tau_m)$ is the fractional population of those nuclei that at the beginning of the mixing time were in site $i$ and at the end in site $j$, while $S_{i,j}(t_1,t_2)$ is the contribution of these nuclei to the total time domain signal. Fourier transformation of $S(t_1,t_2;\tau_m)$ with respect to both $t_1$ and $t_2$ yields the spectrum

$$S(\omega_1,\omega_2;\tau_m) = \sum_{i,j} P_{i,j}(\tau_m) S_{i,j}(\omega_1,\omega_2) \qquad (6)$$

consisting of a weighted superposition of the two-dimensional subspectra $S_{i,j}(\omega_1,\omega_2)$. The simulation of two-dimensional ex-

(19) Vanderhart, D. L. *J. Magn. Reson.* **1987**, *72*, 13.

**Table I.** Principal Components of the Chemical Shift Tensors of Bullvalene[a]

| carbon | $\sigma_{iso}$, ppm[b] | $\sigma_{xx}$, ppm[c] | $\sigma_{yy}$, ppm[c] | $\sigma_{zz}$, ppm[c] |
|---|---|---|---|---|
| 1 | 22 | 35 | −7 | −28 |
| 4[d] | 31 | | | |
| 2, 3 | 128 | 95 | 0 | −95 |

[a] Determined from spinning sideband intensities in MAS spectra by using a Herzfeld–Berger analysis.[20] [b] Relative to TMS. [c] Relative to the corresponding $\sigma_{iso}$. [d] No sidebands observed at $\omega_R/2\pi$ = 1 kHz.

change spectra thus requires the calculation of first the $n^2$ subspectra, which arise from exchange between the $n$ distinct sites in the molecule, and second the corresponding fractional populations. For bullvalene, $C_{10}H_{10}$, neglecting translational diffusion, there are 10 distinct sites between which the carbon atoms of a single molecule can switch, all having the same normalized equilibrium population, $P_i^0 = 1/10$. To obtain the $P_{i,j}(\tau_m)$'s for the bullvalene carbon atoms we need to solve the coupled kinetic equations[18]

$$d\mathbf{P}(t)/dt = (k_C\mathbf{K}_C + k_J\mathbf{K}_J)\mathbf{P}(t) \qquad (7)$$

where $\mathbf{P}(t)$ is a vector, the components of which are the populations of the 10 sites, $\mathbf{K}_C$ is the kinetic matrix for the Cope rearrangement, $\mathbf{K}_J$ is the kinetic matrix for the threefold jumps, and $k_C$ and $k_J$ are the corresponding rate constants. In the notation of Figure 1b, with the lines and rows indicated in the order 1A, 1B, ...4, the kinetic matrices are

$$\mathbf{K}_C = \begin{bmatrix} -1 & 0 & 0 & 0 & 0 & 0 & 2/9 & 2/9 & 2/9 & 1/3 \\ 0 & -1 & 0 & 0 & 0 & 0 & 2/9 & 2/9 & 2/9 & 1/3 \\ 0 & 0 & -1 & 0 & 0 & 0 & 2/9 & 2/9 & 2/9 & 1/3 \\ 0 & 0 & 0 & -7/9 & 2/9 & 2/9 & 1/9 & 1/9 & 1/9 & 0 \\ 0 & 0 & 0 & 2/9 & -7/9 & 2/9 & 1/9 & 1/9 & 1/9 & 0 \\ 0 & 0 & 0 & 2/9 & 2/9 & -7/9 & 1/9 & 1/9 & 1/9 & 0 \\ 2/9 & 2/9 & 2/9 & 1/9 & 1/9 & 1/9 & -1 & 0 & 0 & 0 \\ 2/9 & 2/9 & 2/9 & 1/9 & 1/9 & 1/9 & 0 & -1 & 0 & 0 \\ 2/9 & 2/9 & 2/9 & 1/9 & 1/9 & 1/9 & 0 & 0 & -1 & 0 \\ 1/3 & 1/3 & 1/3 & 0 & 0 & 0 & 0 & 0 & 0 & -1 \end{bmatrix}$$

and

$$\mathbf{K}_J = \begin{bmatrix} -1 & 1/2 & 1/2 & 0 & 0 & 0 & 0 & 0 & 0 & 0 \\ 1/2 & -1 & 1/2 & 0 & 0 & 0 & 0 & 0 & 0 & 0 \\ 1/2 & 1/2 & -1 & 0 & 0 & 0 & 0 & 0 & 0 & 0 \\ 0 & 0 & 0 & -1 & 1/2 & 1/2 & 0 & 0 & 0 & 0 \\ 0 & 0 & 0 & 1/2 & -1 & 1/2 & 0 & 0 & 0 & 0 \\ 0 & 0 & 0 & 1/2 & 1/2 & -1 & 0 & 0 & 0 & 0 \\ 0 & 0 & 0 & 0 & 0 & 0 & -1 & 1/2 & 1/2 & 0 \\ 0 & 0 & 0 & 0 & 0 & 0 & 1/2 & -1 & 1/2 & 0 \\ 0 & 0 & 0 & 0 & 0 & 0 & 1/2 & 1/2 & -1 & 0 \\ 0 & 0 & 0 & 0 & 0 & 0 & 0 & 0 & 0 & 0 \end{bmatrix} \qquad (8)$$

Note that in writing $\mathbf{K}_C$ it is assumed that the three bonds in the three-membered ring are equally likely to break during the bond shift process and that the reorientation that follows the rearrangement brings the new bridgehead carbon to the original site of carbon 4 and the newly formed three-membered ring to the original positions of the three carbons 1 with equal probability for all three symmetry-related orientations. Solution of eq 7 with the initial equilibrium populations gives

$$P_{i,j}(\tau_m) = (1/10)\{\exp[(k_C\mathbf{K}_C + k_J\mathbf{K}_J)\tau_m]\}_{i,j} \qquad (9)$$

which can be solved numerically for any $k_C$ and $k_J$.

Neglecting relaxation effects, the subspectra $S_{i,j}(\omega_1,\omega_2)$ in eq 6 are given by

$$S_{i,j}(\omega_1,\omega_2) = \sum_{M,N} \delta(\omega_1 - \omega_L\Delta\sigma^i_{iso} - M\omega_R)\,\delta(\omega_2 - \omega_L\Delta\sigma^j_{iso} - N\omega_R)I^{i,j}_{M,N} \qquad (10)$$

where $I^{i,j}_{M,N}$ is the intensity of the exchange cross peak located at the frequency coordinates ($\omega_1 = \omega_L\sigma^i_{iso} + M\omega_R$, $\omega_2 = \omega_L\sigma^j_{iso} + N\omega_R$). Formulas for the $I^{i,j}_{M,N}$'s are given in paper 1. Their calculation requires a detailed knowledge of the magnitudes and orientations of the chemical shift tensors of the different carbon atoms in a molecular-fixed coordinate system. The principal components of these tensors were estimated by using a Herzfeld–Berger analysis[20] from one-dimensional spectra recorded at

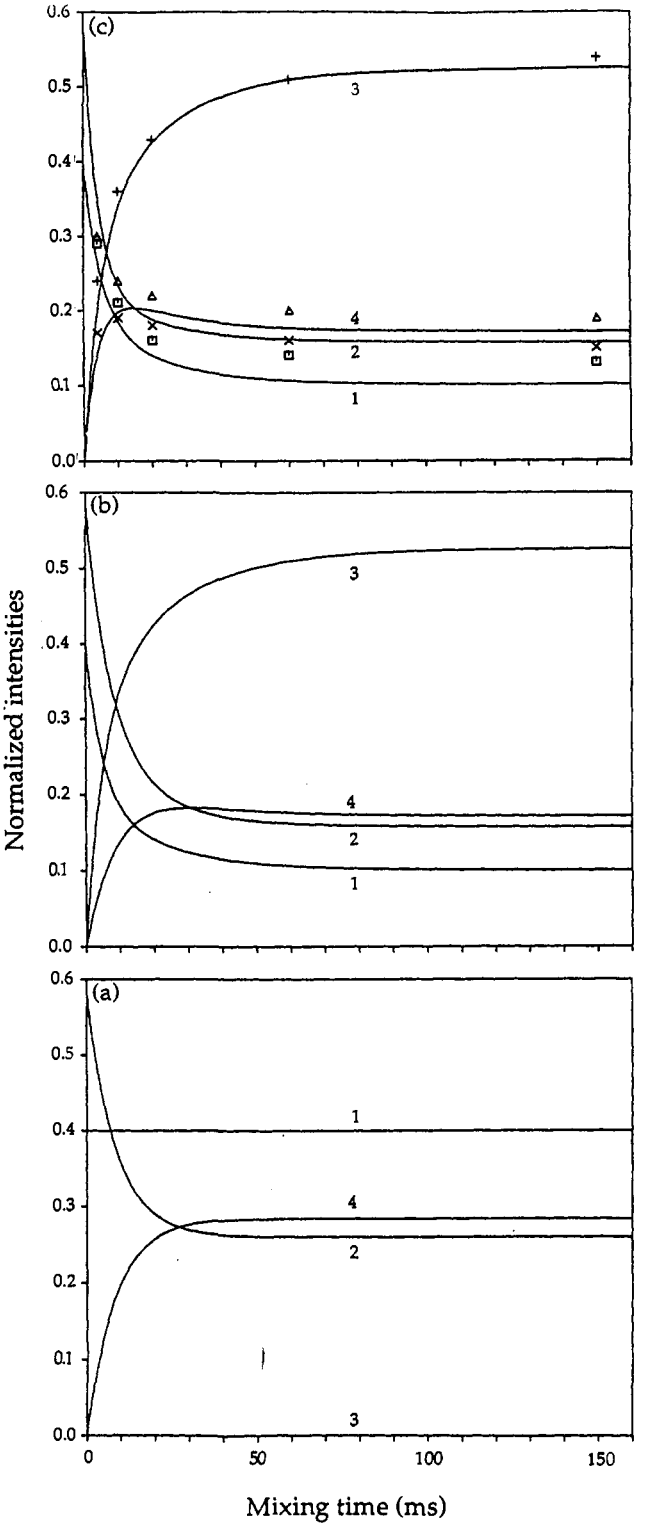


Figure 7. Calculated intensities for the four groups of peaks as defined in the text and in Figure 6 as a function of mixing time for (a) $k_J$ = 80 $s^{-1}$, $k_C$ = 0 $s^{-1}$, (b) $k_J$ = 0 $s^{-1}$, $k_C$ = 120 $s^{-1}$, and (c) $k_J$ = 80 $s^{-1}$, $k_C$ = 120 $s^{-1}$. The experimental points of Figure 6 (with the same symbols) are also included in part c of this figure.

(20) Herzfeld, J.; Berger, A. E. *J. Chem. Phys.* **1980**, *73*, 6021.

**Table II.** Classification of the 100 Two-Dimensional Subspectra $S_{i,j}(\omega_i,\omega_j)$ of Bullvalene

| class | initial and final sites | representative subspectrum | peak intensities | peak frequencies | no. of equivalent subspectra |
|---|---|---|---|---|---|
| A′ | $i$ = 1A, 1B, 1C<br>$j$ = 1A, 1B, 1C | $S_{1,1}(\omega_1,\omega_2)$ | $I^{1,1}{}_{0,0} = 1$ | $\omega_1 = \omega_L\sigma_{iso}{}^1$<br>$\omega_2 = \omega_L\sigma_{iso}{}^1$ | 9 |
| A″ | $i$ = 4<br>$j$ = 4 | $S_{4,4}(\omega_1,\omega_2)$ | $I^{4,4}{}_{0,0} = 1$ | $\omega_1 = \omega_L\sigma_{iso}{}^4$<br>$\omega_2 = \omega_L\sigma_{iso}{}^4$ | 1 |
| A‴[a] | $i$ = 1A, 1B, 1C<br>$j$ = 4 | $S_{1,4}(\omega_1,\omega_2)$ | $I^{1,4}{}_{0,0} = 1$ | $\omega_1 = \omega_L\sigma_{iso}{}^1$<br>$\omega_2 = \omega_L\sigma_{iso}{}^4$ | 3 + 3 |
| B′[a] | $i$ = 1A, 1B, 1C<br>$j$ = 2A, 2B, 2C, 3A, 3B, 3C | $S_{1,2A}(\omega_1,\omega_2)$ | $I^{1,2A}{}_{0,N}$ | $\omega_1 = \omega_L\sigma_{iso}{}^1$<br>$\omega_2 = \omega_L\sigma_{iso}{}^2 + N\omega_R$ | 18 + 18 |
| B″[a] | $i$ = 4<br>$j$ = 2A, 2B, 2C, 3A, 3B, 3C | $S_{4,2A}(\omega_1,\omega_2)$ | $I^{4,2A}{}_{0,N} = I^{1,2A}{}_{0,N}$ | $\omega_1 = \omega_L\sigma_{iso}{}^4$<br>$\omega_2 = \omega_L\sigma_{iso}{}^2 + N\omega_R$ | 6 + 6 |
| B‴ | $i$ = 2A, 3A; 2B, 3B; 2C, 3C<br>$j$ = 2A, 3A; 2B, 3B; 2C, 3C | $S_{2A,2A}(\omega_1,\omega_2)$ | $I^{2A,2A}{}_{N,N} = I^{1,2A}{}_{0,N}$ | $\omega_1 = \omega_L\sigma_{iso}{}^2 + N\omega_R$<br>$\omega_2 = \omega_L\sigma_{iso}{}^2 + N\omega_R$ | 12 |
| C[a] | $i$ = 2A, 3A; 2B, 3B; 3C, 3C<br>$j$ = 2B, 3B; 2C, 3C; 3A, 3A | $S_{2A,2B}(\omega_1,\omega_2)$ | $I^{2A,2B}{}_{M,N}$ | $\omega_1 = \omega_L\sigma_{iso}{}^2 + M\omega_R$<br>$\omega_2 = \omega_L\sigma_{iso}{}^2 + N\omega_R$ | 12 + 12 |

[a] The classes A‴, B′, B″, and C each consist of two subspectra related to each other by a reflection along the main diagonal. Only one of the subspectra is indicated in the table; the second can be obtained by interchanging $\omega_1$ and $\omega_2$.

low spinning frequencies. The results of this analysis are shown in Table I. No spinning sidebands were observed for carbon 4 even at as low a spinning rate as 1 kHz, indicating that its overall chemical shift anisotropy is less than 25 ppm. Since the spinning frequency used for our two-dimensional measurements was 2.8 kHz, no sidebands were observed for either of the aliphatic carbon atoms and their shift anisotropies can be completely neglected. The Herzfeld–Berger analysis does not provide information about the orientation of the principal directions of the chemical shift tensors in the molecular frame and so we shall make the following assumptions. First, we assume that carbons 2 and 3 in each wing of the bullvalene molecule are completely magnetically equivalent with identical directions and magnitudes of all three principal components of their chemical shift tensors. Second, in analogy with literature data,[21] we assume that the intermediate component of the principal axes system (PAS), $\sigma_{yy}$, lies along the double bond direction associated with the corresponding carbon atom and the most shielded component, $\sigma_{zz}$, is oriented perpendicular to the plane of the wing. The third principal component, $\sigma_{xx}$, must then lie in the plane of the wing perpendicular to the double bond. For a molecule-fixed frame (MF) we choose a coordinate system 1, 2, 3 with the 3-axis along the molecular $C_3$ symmetry axis, the 1-axis in the plane of wing A perpendicular to 3, and the 2-axis perpendicular to both, completing a right-handed system. From the molecular structure of bullvalene[9] an average value of $\theta$ = 14.2° for the angle between the molecular $C_3$ axis and the double bond direction can be calculated. Assuming perfect $C_3$ symmetry, the elements $\sigma_{n,m}$ ($n$, $m$ = 1, 2, 3) of the chemical shift tensors in the molecule-fixed frame are then related to the principal components by the rotation

$$\sigma(\mathrm{MF}) = R(\theta,\phi)\sigma(\mathrm{PAS})R^{-1}(\theta,\phi) \qquad (11)$$

where

$$\sigma(\mathrm{PAS}) = \begin{bmatrix} \sigma_{xx} & 0 & 0 \\ 0 & \sigma_{zz} & 0 \\ 0 & 0 & \sigma_{yy} \end{bmatrix} \qquad (12)$$

and

$$R(\theta,\phi) = \begin{bmatrix} \cos\theta\cos\phi & \sin\phi & -\sin\theta\cos\phi \\ -\cos\theta\sin\phi & \cos\phi & \sin\theta\sin\phi \\ \sin\theta & 0 & \cos\theta \end{bmatrix} \qquad (13)$$

with $\phi$ = 0°, 120°, and 240° for the olefinic carbons in respectively wings A, B, and C. With these results for the chemical shift tensors, all the required cross-peak intensities can be calculated by using eqs 6–10 of paper 1.

As indicated above, there are $n^2$ = 100 subspectra for bullvalene. However, only $55 = n(n+1)/2$ of these are independent because the subspectrum $S_{i,j}(\omega_1,\omega_2)$ is related to $S_{j,i}(\omega_1,\omega_2)$ by a reflection in the main diagonal of the two-dimensional plane $S_{j,i}(\omega_1,\omega_2) = S_{i,j}(\omega_2,\omega_1)$. The number of subspectra that need to be calculated is further reduced by neglect of the chemical shift anisotropy of the aliphatic carbons 1 and 4, the assumption of complete magnetic equivalence of carbons 2 and 3 in each wing of the molecule, and the overall threefold symmetry of bullvalene. These symmetry relations and assumptions reduce the set of subspectra to a manageable seven distinct ones. They are listed in Table II where their properties are summarized. Examination of this table shows that in practice only two sets of peak intensities need actually be computed, namely, $S_{1,2A}(\omega_1,\omega_2)$ and $S_{2A,2B}(\omega_1,\omega_2)$. All other subspectra either consist of a single line at the isotropic shift with unit intensity or are equivalent to one of these two (except for a shift in the frequency coordinates). Note that the peak intensities associated with $S_{1,2A}(\omega_1,\omega_2)$ are identical with the corresponding Herzfeld–Berger intensities. Since at most two sidebands are observed on each side of the olefinic center band, we need only calculate five intensities of the type $I_{0,N}{}^{1,2A}$ and 15 of the type $I_{M,N}{}^{2A,2B}$ ($N, M$ = −2, −1, 0, 1, 2). The numerical values obtained by using the parameters discussed for bullvalence are summarized in Table III. By a combination of these results with those for the $P_{i,j}(\tau_m)$'s of eq 9 the whole two-dimensional spectrum can be simulated as a function of the mixing time.

**Table III.** Calculated Cross-Peak Intensities for the Subspectra of Classes B and C

| $M$ \ $N$ | −2 | −1 | 0 | 1 | 2 |
|---|---|---|---|---|---|
| Cross-Peak Intensities, $I^{1,2A}{}_{0,N} = I^{4,2A}{}_{0,N} = I^{2A,2A}{}_{0,N}$ in Subspectra of Class B | | | | | |
| | 0.09 | 0.24 | 0.31 | 0.24 | 0.09 |
| Cross-Peak Intensities, $I^{2A,2B}{}_{M,N}$, for Subspectra of Class C | | | | | |
| −2 | 0.0 | 0.0 | 0.030 | 0.035 | 0.015 |
| −1 | 0.0 | 0.054 | 0.074 | 0.063 | 0.036 |
| 0 | 0.03 | 0.074 | 0.061 | 0.072 | 0.031 |
| 1 | 0.035 | 0.063 | 0.072 | 0.052 | 0.0 |
| 2 | 0.015 | 0.036 | 0.031 | 0.0 | 0.0 |

### Comparison of Experimental and Calculated Peak Intensities

A conspicuous feature of the experimental results plotted in Figure 6 is the nonmonotonous dependence on the mixing time of the cross-peak intensities of group 4. Such a behavior reflects the occurrence of two independent processes, the Cope rearrangement, and the threefold jumps. These cross peaks that link the different spinning sidebands of the olefinic carbons are clearly most sensitive to the relative rates of the two processes. While the threefold jumps can only create such cross peaks, the Cope rearrangement can also reduce them by "sharing" their intensities with the other cross peaks (group 3). To illustrate this effect, we show in Figure 7 plots of the calculated intensities of the four groups of peaks for three situations: (a) pure threefold jumps with $k_J$ = 80 s$^{-1}$, (b) pure Cope rearrangement/reorientation with $k_C$

(21) Veeman, W. S. *Prog. Nucl. Magn. Reson. Spectrosc.* **1984**, *16*, 193.

= 120 $s^{-1}$, and (c) the combination of (a) and (b). Clearly in (a) only groups 2 and 4 are affected; peaks in groups 1 and 3 are not affected by the jump process because of our neglect of the shift anisotropy of the aliphatic carbons. In (b) all the peaks are affected because the Cope rearrangement intermixes all carbon atoms in the molecule. However, when both the threefold jumps and the Cope rearrangement take place simultaneously marked nonmonotonous behavior can occur as demonstrated in part c.

The rate constants $k_J$ and $k_C$ used to calculate the plots in Figure 7c were chosen so as to mimic the behavior of the experimental results, which are also included in this part of the figure with the same set of symbols as for Figure 6. Note that the major features of the four curves occur in the first 30 ms of the plots and that only when both the effect of the threefold jump and the Cope rearrangement are included does the theory resemble the experimental data in this region. In fact the rate constants used for the calculations also fall close to those estimated from the one-dimensional spectra in Figure 4. The fit could no doubt be improved by varying $k_J$ and $k_C$ and by including corrections to account for possible small differences in the cross-polarization efficiency of the different carbon atoms, longitudinal relaxation during the mixing time, and even slow spin diffusion. In view of the uncertainty associated with the peak volume integration we have not pursued a more extensive analysis. We feel, however, that the quality of the fit obtained with the approximate rate constants and without further refinement is quite satisfactory.

Since the activation energy of the threefold jumps is higher than for the Cope rearrangement (Figure 4), the ratio $k_J/k_C$ decreases with decreasing temperature and the competing effect of the two processes becomes less pronounced. This was clearly observed in results obtained at −20 °C, where the maximum in the total intensity of the group 4 peaks with respect to the mixing time became flatter. On the other hand, above −10 °C, exchange broadening sets in, rendering the recording of such two-dimensional spectra impossible.

## Summary and Conclusions

The results reported here on the dynamic processes in solid bullvalene are in good agreement with the earlier deuterium NMR study of a single crystal.[12] In particular, both the deuterium and carbon-13 studies indicate the occurrence of two independent dynamic processes: the symmetric threefold jumps and a concerted Cope rearrangement/reorientation process. Both deuterium and carbon-13 NMR studies have been used extensively to investigate dynamic processes in solids. The former approach has the disadvantage that it requires specific chemical labeling of the compound of interest because of the low natural abundance of deuterium. The sensitivity of natural abundance carbon-13 NMR spectroscopy is normally acceptable but static samples give complicated spectra due to the overlap of signals from different carbon atoms. The low spinning rate carbon-13 MAS experiment employed here for the case of bullvalene provides increased spectral resolution, while the surviving sidebands contain information about the chemical shift anisotropy and thus about reorientation processes. Specific chemical labeling is unnecessary. When applicable this approach should be the method of choice for studying dynamic processes in solids.

**Acknowledgment.** We thank Prof. G. Schröder for a generous gift of the bullvalene sample used in our experiments. J.J.T. thanks the Science and Engineering Research Council of Great Britain for a NATO postdoctoral fellowship. Z.L. thanks the Minerva Foundation for a visiting scientist fellowship.

**Registry No.** Bullvalene, 1005-51-2.

# Diastereoselective Reactions of Tungsten $\eta^2$-Propargyl Complexes with Alkyl Halides and Aldehydes

**M. A. Collins, S. G. Feng, P. A. White, and J. L. Templeton***

*Contribution from the Department of Chemistry, University of North Carolina, Chapel Hill, North Carolina 27599.* *Received February 28, 1991*

**Abstract:** Deprotonation of the alkyne methyl group in Tp′(CO)(I)W(PhC≡$CCH_3$) [Tp′ = hydridotris(3,5-dimethylpyrazolyl)borate] produces a nucleophilic propargyl synthon. Reaction of the complex anion with MeI or $PhCH_2Br$ yields an elaborated alkyne and avoids the propargyl/allenyl regiochemical control problem. Deprotonation of Tp′(CO)(I)W(PhC≡$CCH_2$Me) followed by benzylation produces a single diastereomer as determined by $^1$H NMR, while methylation of the anion formed from Tp′(CO)(I)W(PhC≡$CCH_2$Bz) yields the opposite diastereomer. Pivaldehyde or benzaldehyde adds to the coordinated $\eta^2$-propargyl carbanion, Li[Tp′(CO)(I)W($\eta^2$-PhC=C=CHMe)], to form alcohol products. Conversion to a coordinated enyne was achieved for the benzaldehyde adduct by first forming the mesyl derivative and then eliminating $HOSO_2Me$ to yield Tp′(CO)(I)W(PhC≡CCMe=CHPh).

## Introduction

Alkynes are versatile organic building blocks.[1] Although alkynes are of demonstrated value in organic synthesis, regiocontrol of electrophilic addition to propargyl carbanion equivalents has been difficult to achieve with classical metalated propargyl reagents (eq 1).[2]

$$RC{\equiv}CCH_3 \xrightarrow{\text{base}} RC{\equiv}C{-}\bar{C}H_2 \leftrightarrow R\bar{C}{=}C{=}CH_2 \quad (1)$$

In 1968, Corey and Kirst reported a method for propargylating an alkyl halide by reacting the halide with lithio-1-trimethylsilylpropyne.[3] Alkylation occurred almost exclusively at the propargyl site to yield alkyne products as the trimethylsilyl group limited alkylation at the alkyne carbon. Thus allene products were avoided; the trimethylsilyl protecting group was easily removed.

Nicolas has achieved regiocontrol of nucleophilic addition to a cationic propargyl synthon through coordination of an alkyne

(1) Viehe, H. G., Ed. *Chemistry of Acetylenes*; Marcel Dekker: New York, 1969.

(2) Klein, J. In *The Chemistry of the Carbon-Carbon Triple Bond, Part I.*; Patai, S., Ed.; John Wiley & Sons: New York, 1978; pp 343–379.

(3) (a) Corey, E. J.; Kirst, H. A. *Tetrahedron Lett.* **1968**, *48*, 5041. (b) Corey, E. J.; Kirst, H. A.; Katzenellenbogen, J. A. *J. Am. Chem. Soc.* **1970**, *92*, 6314. (c) Ireland, R. E.; Dawson, M. I.; Lipinski, C. A. *Tetrahedron Lett.* **1970**, *26*, 2247.

0002-7863/92/1514-3771$03.00/0 